BEAM LOADING ANALYSIS OF A TRANSFORMER-COUPLED RF CAVITY

S. Bartalucci, R. Garoby, A. Riche and A. Susini

CERN, 1211 GENEVA 23, Switzerland

1. Introduction

Coherent dipole longitudinal instabilities have been observed in the Electron-Positron Accumulation Ring (EPA), which is part of the LEP injector chain. These instabilities turn into a strong limitation upon the maximum beam current, depending on RF cavity voltage and tuning angle. Although the nominal performances of the machine are not affected, as far as the operation of the LEP injector chain is concerned, a study of beam loading effects seems worthwhile, because: i) it might be necessary to accumulate up to 4 times the nominal intensity for LEP injection, ii) it was foreseen to reduce the cavity voltage for optimum injection to the PS, iii) owing to the rather unconventional design of the RF cavity, one might expect the intensity limits to be different from those predicted by classical Robinson's criterion.

In this paper a transformer-coupled resonator model for the EPA RF cavity is presented, and a detailed analysis of its beam loading stability is performed. The results are compared both with Robinson's criterion and with some measurements taken during EPA running-in.

2. The cavity model

The EPA RF system [1] consists of an accelerating cavity coupled through a magnetic loop to an amplifier cavity where the power tetrode is located. The equivalent lumped circuit of this system is shown in Fig. 1, together with the usual phasor diagram. The power tube is represented by a current generator with its plate resistance R_p added in parallel. The beam is also represented by a current generator at the fundamental frequency 19.1 MHz, whose amplitude is twice the DC beam current (valid for typical EPA bunch lengths). In the following we shall adopt the notation used by Pedersen [2].

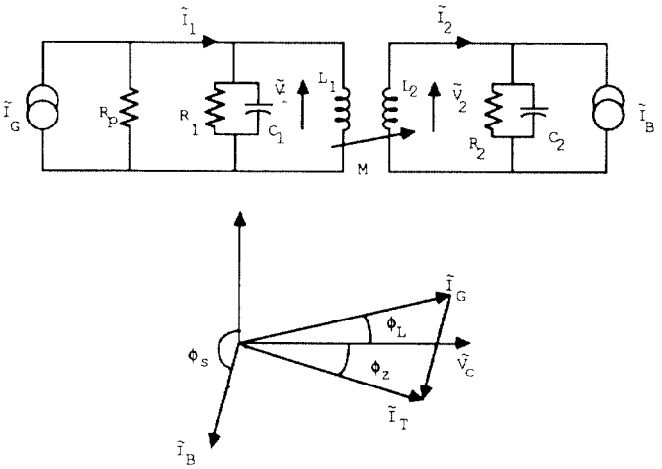

Fig. 1 - Equivalent circuit and phasor diagram

Using Kirchhoff's laws the following complex quantities can be calculated:

$\tilde{Z}_{11} = (\frac{\tilde{V}_1}{\tilde{I}_1})_{I_B=0}$, i.e. the impedance seen by the power generator,

$\tilde{Z}_{21} = (\frac{\tilde{V}_2}{\tilde{I}_1})_{I_B=0}$, i.e. the anode impedance transformed to the accelerating gap, $\tilde{\tau} = (\frac{\tilde{V}_2}{\tilde{V}_1})_{I_B=0}$, i.e. the voltage step-up (transformation ratio) between the anode and the gap and $\tilde{Z}_{22} = (\frac{\tilde{V}_2}{\tilde{I}_B})_{I_G=0}$, the gap impedance (as seen by the beam).

We are interested in the transmission from small modulations of I_B to the beam induced voltage V_B, that is, in

$$\tilde{Z}_{22} = \frac{s}{C_2} \frac{s^2 + \alpha_1 s + \frac{\omega_1^2}{1-k^2}}{s^4 + s^3(\alpha_1+\alpha_2) + s^2(\alpha_1\alpha_2 + \frac{\omega_1^2+\omega_2^2}{1-k^2}) + s(\frac{\alpha_1\omega_2^2+\alpha_2\omega_1^2}{1-k^2}) + \frac{(\omega_1\omega_2)^2}{1-k^2}} \quad (1)$$

where $s = j\omega$. The damping coefficients $\alpha_{1,2} = \frac{1}{R_{1,2}C_{1,2}}$, the mutual inductance coefficient $k = \frac{M}{\sqrt{L_1 L_2}}$ and the resonant frequencies $\omega_{1,2} = \frac{1}{\sqrt{L_{1,2}C_{1,2}}}$ of the primary and secondary circuits are derived from low-level measurements.

A typical set of parameters is reported in Table I.

The plate resistance has been estimated from the tube characteristics (SIEMENS RS 1084 tetrode) and added in parallel on the generator side. The cavity shunt impedance R_s has not been directly measured, but it is estimated as $R_s = Zn \cdot Q$, where the characteristic impedance $Zn = 41\ \Omega$ was calculated by SUPERFISH and the loaded quality factor $Q = 3446$ was measured with a Network Analyzer.

Table I - Cavity parameters

$f_1 = \frac{\omega_1}{2\pi} = 16857.0$ kHz, $Q_1 = 1000$, $Zn_1 = 45\ \Omega$

$f_2 = \frac{\omega_2}{2\pi} = 19029.34$ kHz, $Q_2 = 6000$, $Zn_2 = 41\ \Omega$

$R_p = 7.2\ k\Omega$, $f_0 = \frac{\omega_0}{2\pi} = 19085.24$ kHz bunch frequency

$\frac{\Omega}{2\pi} = \frac{\omega_0 k}{4\pi} = 335.5$ kHz

The stability analysis of such a system will follow the guidelines of Pedersen's work. For the beam we assume rigid bunches, so its phase transfer function between excitation and beam is:

$$B(s) = \frac{\omega_s^2}{s^2 + \omega_s^2}$$

The impedance (1) has been used to calculate the transfer functions $G^B{}_{pp}(s)$ and $G^B{}_{pa}(s)$ for transmission of amplitude and phase

modulations through the cavity, which are defined in Appendix A.

The characteristic equation is:

$$1 - B(s) \cdot \left(G^{B}_{pp}(s) + \tan\phi_s\, G^{B}_{pa}(s)\right) = 0 \qquad (2)$$

and we know that the system is unstable if, and only if, the characteristic equation has roots with positive real part.

By inspection of the above formulae, it is easily recognized that this equation will be of 10th degree in s, with very complicated coefficients, making the analytical solution impossible even with the help of symbolic programming. Therefore a program has been written to perform this calculation numerically (see Appendix B).

3. Results and comparison with measurements

First we have considered the case where the generator current I_G is constant. If the power tube is assumed to be an ideal current generator, this corresponds to the experiment where a constant excitation is applied to the control grid of the tube. Furthermore the tuning loop is disabled in order to keep the phase angle ϕ_Z of the cavity impedance constant. The parameters which enter eq. (2), are I_G, I_B, ϕ_Z, ϕ_S and ϕ_L. These two last angles are no longer constant during accumulation, so we used the steady state conditions as derived from the phasor diagram:

$$I_G \cos\phi_L = \frac{V_c}{R_S} + I_B \sin\phi_s,\quad \tan\phi_L = \frac{\tan\phi_z - \dfrac{I_B R_s}{V_c}\cos\phi_s}{1 + \dfrac{I_B R_s}{V_c}\sin\phi_s}$$

with $\phi_s = \arccos\left(-\sqrt{1-\left(\dfrac{U_0}{eV_c}\right)^2}\right)$ and U_0 is the synchrotron radiation loss per turn at 500 MeV. From these 3 eqs. we eliminate ϕ_s and ϕ_L and we get a 4th order polynomial (see Appendix C) in V_c which is analytically solvable. In this way we determine the stability for any ϕ_z = const. trajectory in the (ϕ_L, I_B) plot by applying the Routh-Hurwitz criterion to the characteristic equation.

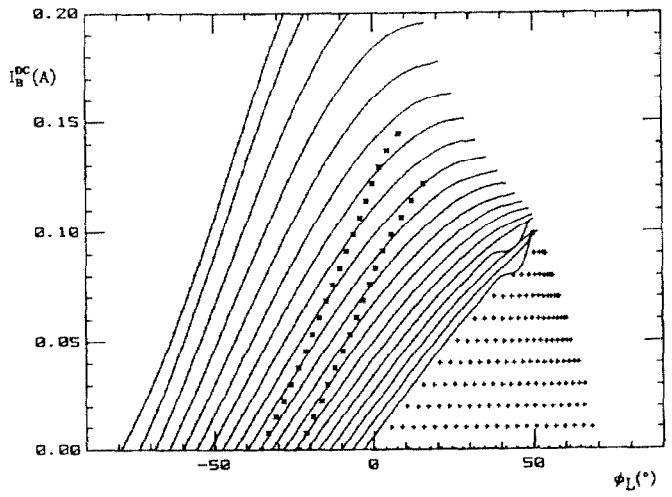

Fig. 2 -Stable trajectories for the transformer-coupled cavity:
* measured trajectories, + Robinson instability.

An example is shown in Fig. 2. The stable trajectories are described by solid lines, which are stopped when the polynomial has no longer any real solution. It happens that the cavity voltage V_c and the beam current I_B corresponding to the end point verify exactly Robinson's condition

$$I_B = \frac{V_c}{R_s}\frac{2\cos\phi_s}{\sin 2\phi_z}$$ which was established for the single resonator model.

Moreover, the program which applies the Routh-Hurwitz criterion for the verification of the stability, finds the end points of all the trajectories of Fig. 2 always unstable.

Two measured curves of I_B versus ϕ_L are also shown in Fig. 2. Other measurements have shown that there is a systematic error on the ϕ_L values, probably due to some non-linearity in the power tube.

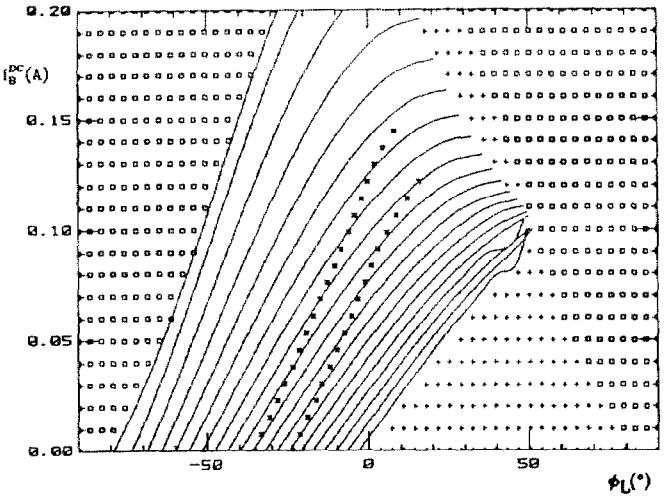

Fig. 3 - Comparison of the two models.

In Fig. 3 the instability zones for the single resonator model are displayed, as calculated by the program, together with the stable trajectories of Fig. 2. The areas shaded with + are unstable according to the Routh-Hurwitz criterion, while those shaded with squares are forbidden by power limits.

Looking at Fig. 3 the only difference between the two models would appear if the instability limit were occurring before the end of the trajectory. This is not the case for the parameters of EPA cavity.

There is a remarkable good agreement between the computed and the experimental curves if we plot, instead of ϕ_L, the cavity voltage V_c against the beam current as in Fig. 4. This is a confirmation of the validity of our model, since the voltage measurement was cross-checked by various means.

We have also investigated the stability of the transformer-coupled system when the cavity voltage is given. In Fig. 5 the trajectories at V_c = 10 kV and constant tuning angle are displayed together with the instability domains. The Robinson limits are superimposed and show good agreement.

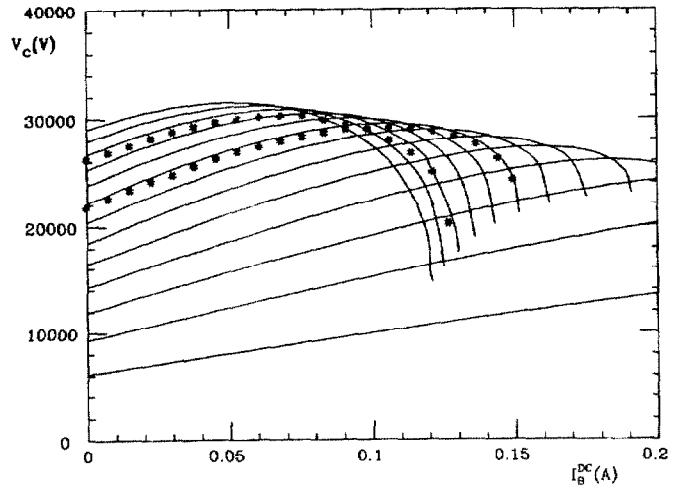

Fig. 4 - Trajectories in the (Vc, I_B^{DC}) plane: - solid lines for the transformer-coupled cavity, * measured trajectories.

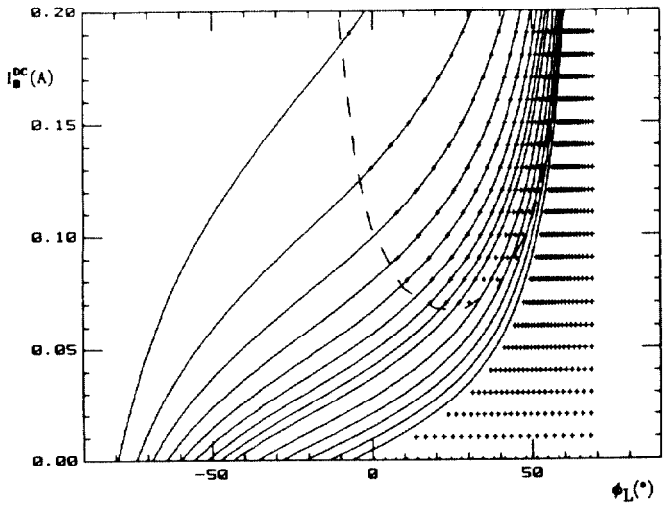

Fig. 5 - Stability plot for the case V_c = 10 kV: + Robinson instability, -- dashed line: theoretical limit, – solid lines: trajectories.

Conclusions

The two-resonator model was introduced as a possible explanation of the observed beam intensity limits in EPA. As shown in Fig. 4 these limits are very close to the thoretical predictions. These predictions appear to be almost identical to those of the single resonator model as shown in Fig. 3, at least for the EPA cavity parameters, where the two resonance peaks are about 2 MHz apart.

Acknowledgements

We thank F. Pedersen for many helpful discussions and suggestions. The constant encouragement and support of J.P. Delahaye and K. Huebner are gratefully acknowledged. Miss M.C. D'Amato is thanked for her skilful technical assistance.

References

(1) S. Bartalucci, M. Bell, F. Caspers, K. Huebner, P. Marchand, A. Susini and R. Poirier, Proc. of the 1987 IEEE Particle Accelerator Conference, Washington (1987) 1791.
(2) F. Pedersen, IEEE Trans. Nucl. Sci. NS-22 (1975) 1906 and unpublished note.

APPENDIX A - Transfer functions through cavity

Z being given by eq.(1)

$$G_s(s) = \frac{1}{2}\left[\frac{Z(s+j\omega_c)}{Z(j\omega_c)} + \frac{Z(s-j\omega_c)}{Z(-j\omega_c)}\right]$$

$$G_c(s) = \frac{j}{2}\left[\frac{Z(s+j\omega_c)}{Z(j\omega_c)} - \frac{Z(s-j\omega_c)}{Z(-j\omega_c)}\right]$$

with $U = I_G/I_B$ and $\phi = \phi_s - \phi_L + \frac{\pi}{2}$

$$G_{pp}^B = [G_s(s)\,(1 + U\cos\phi) - G_c(s)\,U\sin\phi] \,/\, [1 + U^2 + 2U\cos\phi]$$

$$G_{pa}^B = [G_s(s)\,U\sin\phi + G_c(s)\,(1 + U\cos\phi)] \,/\, [1 + U^2 + 2U\cos\phi]$$

APPENDIX B - Calculations of the coefficients of the characteristic equation

The characteristic equation results as a linear combination of terms $s^n \cdot N(s + s_k) \cdot D(s + s_l)$, where s_k and s_l are $j\omega_c$ or $-j\omega_c$, n is 0 or 2, and N and D are the 3th and 4th order polynomials found in $Z_{22} = N/D$ (eq. 1). It is not difficult to calculate the coefficients of s^m, by summing all $n_k s^k d_l s^l s^n$ such that k+l+n = m, and, further, to add the coefficients coming from all the N·D products.

APPENDIX C - Polynomial in V_c

$$\left[\left(\frac{V_c}{R_s\cos\phi_z}\right)^2\right]^2 + 2\left(\frac{V_c}{R_s\cos\phi_z}\right)^2\left[2\,I_B\frac{U_0}{R_s} + I_B^2 - I_G^2 - 2\,I_B^2\sin^2\phi_z\right] +$$

$$+ \left[2\,I_B\frac{U_0}{R_s} + (I_B^2 - I_G^2)\right]^2 + \left[2\,\frac{U_0}{R_s}I_B\tan\phi_z\right]^2 = 0$$